

Quantum Percolation and Plateau Transitions in the Quantum Hall Effect

Dung-Hai Lee,⁽¹⁾ Ziqiang Wang,⁽²⁾ and Steven Kivelson⁽³⁾

⁽¹⁾IBM Research Division, T. J. Watson Research Center, Yorktown Heights, New York 10598

⁽²⁾Center for Materials Science and Theoretical Division T-11, Los Alamos National Laboratory, Los Alamos, New Mexico 87545

⁽³⁾Department of Physics, University of California at Los Angeles, Los Angeles, California 90024-1547

(Received 8 March 1993)

We introduce a simple model of quantum percolation and analyze it numerically using transfer matrix methods. A central point of this paper is that *both integer and fractional plateau transitions in the quantum Hall effect are due to quantum percolation*. Within this model, we obtained the localization length exponent $\nu=2.4 \pm 0.2$, the dynamical exponent $z=1$, and the scaling functions for the conductivity tensor for both the integer and the fractional transitions. We show that our results agree extremely well with the experimental results for the integer plateau transition obtained by McEuen *et al.*

PACS numbers: 73.40.Hm, 05.30.-d, 73.50.Jt

When a sufficiently clean two-dimensional electron gas is placed in a strong magnetic field, it exhibits the quantum Hall effect [1]. In his seminal work [2], Laughlin identified the ideal states that support this behavior as the incompressible quantum liquids (or Hall liquids). Recently, in an attempt to develop a global view of the spin-polarized quantum Hall effect, Kivelson, Lee, and Zhang (KLZ) [3(a)] have proposed a schematic phase diagram which exhibits the interconnection among various Hall liquids. In this paper, we address the critical properties of the quantum phase transitions between adjacent quantum Hall liquid phases.

Experimentally, these transitions are manifested as plateau transitions in which, over a narrow interval of magnetic field ΔB , ρ_{xy} changes from one quantized value to another. Following a suggestion of Pruisken [4(a)], Wei *et al.* [5(a)] carefully measured ΔB of the integer plateau transitions and showed that as $T \rightarrow 0$, $\Delta B \propto T^{\kappa}$ with $\kappa=0.42 \pm 0.02$. From a simple finite-size-scaling analysis it follows that $\kappa=1/\nu z_T$ where ν is the localization length exponent and z_T (which is conventionally called $2/p$ [4(a)]) is a thermal exponent which determines the finite size that cuts off the critical fluctuations. Similar experiments have also been performed in the fractional regime [5(b)]. The results showed that κ is the same for the integer and the fractional plateau transitions and hence suggest that they belong to the same universality class. Finally, Koch *et al.* [5(c)] performed similar measurements in narrow channels and determined ν ($\nu=2.3 \pm 0.1$) directly.

Pruisken *et al.* have provided an interesting theoretical framework for thinking about the integer plateau transitions [4(b)]. More recently, considerable progress in understanding the integer transitions has been made on the basis of numerical studies of noninteracting electrons in the lowest Landau level. In these studies a localization length exponent $\nu=2.37 \pm 0.13$ [6(a)] and universal critical conductivities [3] $\sigma_{xy}^c=(0.5 \pm 0.05)e^2/h$ and $\sigma_{xx}^c=(0.5 \pm 0.05)e^2/h$ [6(b)] were found for a variety of models with finite-range impurity scattering. It remains unclear how to generalize these results to include Coulomb interactions and the fractional quantum Hall

effect.

In this paper, we study a generalized version of the network model of quantum percolation introduced by Chalker and Coddington [7(a)]. Our generalization is to allow disorder in the strength of quantum tunneling at each node of the network. We have solved this model numerically using transfer matrix methods and found ν and the scaling functions for the conductivities. Our values of ν ($=2.43 \pm 0.18$) and the critical conductivities agree with the results in Ref. [6]. Since in two dimensions we generally expect critical conductivities to be universal [8], we regard both of these results as evidence that all the models considered are in the same universality class, and that quantum percolation governs the plateau transitions. A central point of the present paper is a physical argument which suggests that *all* plateau transitions (in the presence of Coulomb interactions) are due to quantum percolation. For Coulomb interactions, we have also obtained the dynamical exponent $z=1$. Finally, we have compared our results for the conductivities in the scaling regime with the available experimental data [9].

We begin by motivating our model of quantum percolation. Let us consider a random potential which is slowly varying on the scale of the magnetic length, $l_B=\sqrt{\hbar c/eB}$, and let us focus on the transition between a pair of Hall liquids, which we call, respectively, "0" and "1." By convention we will assign labels so that $\sigma_{xy,1} > \sigma_{xy,0}$. (To have a specific example in mind, one can consider the case in which $\sigma_{xy,0}=e^2/3h$ and $\sigma_{xy,1}=2e^2/5h$.) Let us approach the transition from the "1" side so that in real space, the system consists of droplets of the "0" Hall liquid immersed in a background of the "1." (In the presence of Coulomb interaction, one should not think of the "0" and "1" regions as having very different densities; the constraint of charge neutrality on moderate length scales implies that the "1" regions are littered with localized quasiholes and the "0" regions with localized quasiparticles.) As we change the chemical potential, each of the "0" droplets will expand or contract. The smallest unit of charge that can be transferred to a "0" droplet is e^* , the charge of the quasiholes in the "1" liquid (e.g. $e^*=e/5$ in the specific example discussed

above). An added quasihole wave packet propagates along the boundary of the "0" droplet in *one direction* only, with a velocity proportional in magnitude to the gradient of the potential. At low temperatures, the *dissipative* component of the magnetotransport is completely determined by the propagation of these edge quasiholes. The localization length ξ is given by the size of the largest typical droplet. At a fixed density when the magnetic field is low, the "0" Hall droplets are far separated. In that case, all boundaries are finite and the system is macroscopically a "1" Hall liquid. As one increases the magnetic field, the "0" Hall droplets gradually merge. When $B > B_c$, the "0" Hall droplets percolate, and macroscopically the system becomes a "0" Hall liquid.

We now consider the process by which the localization length diverges as $B \rightarrow B_c$. If we ignore quantum tunneling of quasiholes, this is a classical percolation problem. As discussed by Trugman [10] the localization length diverges as $\xi \sim |B - B_c|^{-\nu_c}$, with $\nu_c = \frac{4}{3}$. In reality, quantum tunneling is important whenever the edges of two droplets get close together (i.e., *near a saddle point*).

To study quantum percolation we consider a square lattice of saddle points [11], as shown schematically in Fig. 1, in which the areas marked with "0" and "1" represent the regions occupied by the "0" and "1" Hall liquids, respectively, the squares enclose the saddle points, and the arrows indicate the direction of propagation of the quasiholes. Each saddle point has two incoming and two outgoing edges. Let Z_1 and Z_2 denote the incoming and Z_3 and Z_4 denote the outgoing quasihole probability amplitudes at a single vertex. The quantum tunneling at the saddle point can be summarized by the following matrix equation [7(a)]:

$$\begin{pmatrix} Z_1 \\ Z_3 \end{pmatrix} = \begin{pmatrix} e^{i\phi_1} & 0 \\ 0 & e^{i\phi_2} \end{pmatrix} \begin{pmatrix} \cosh \gamma & \sinh \gamma \\ \sinh \gamma & \cosh \gamma \end{pmatrix} \begin{pmatrix} e^{i\phi_3} & 0 \\ 0 & e^{i\phi_4} \end{pmatrix} \begin{pmatrix} Z_4 \\ Z_2 \end{pmatrix}, \quad (1)$$

where ϕ_i 's account for the random phases of Z_i at the saddle point and γ characterizes the amount of quantum tunneling. The specific form of the matrix in Eq. (1) is dictated by the requirement of *current conservation*, i.e., $|Z_1|^2 + |Z_2|^2 = |Z_3|^2 + |Z_4|^2$ [7(a)]. Classical behavior is recovered in the limits $\gamma \rightarrow 0$, where $(1 \rightarrow 4, 2 \rightarrow 3)$

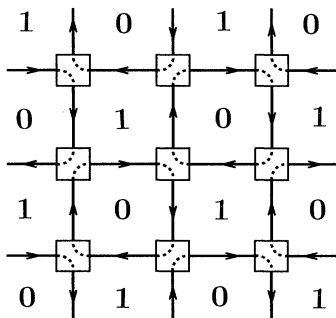


FIG. 1. View of the lattice model of quantum percolation. The dashed curves indicate the direction of propagation in the classical limit when $\gamma=0$ at all saddle points.

with probability unity, and $\gamma \rightarrow \infty$ where $(1 \rightarrow 3, 2 \rightarrow 4)$. The "most quantum mechanical" behavior is realized when $\gamma = \gamma_c = \ln(1 + \sqrt{2})$ where an incoming particle on 1 (or 2) has equal probability to be scattered to 3 or 4. The value of γ is given by $\gamma(\mu) = \gamma_c \exp(\mu - V)$, where μ is the dimensionless chemical potential, and V is a dimensionless random potential distributed in the interval $(-w/2, w/2)$. For finite μ , if we let $W \rightarrow \infty$, γ assumes finite nonzero values with vanishing probability, and hence classical percolation is recovered. Using the matrix in Eq. (1) as the building block we construct the transfer matrix T for a network consisting of $(M \times L)$ saddle points with periodic boundary conditions applied in the M direction. For large enough L the system is self-averaging [7(a)], and the localization length $\xi_M(\mu)$ is given by $\xi_M^{-1}(\mu) = \ln(|\lambda_0(M, L, \mu)|)/L$, where λ_0 is the smallest eigenvalue of T that has $|\lambda_0| \geq 1$.

In the presence of Coulomb interactions, there exists a Lee-Rice length scale ξ_{corr} above which the induced positional (i.e., Wigner crystal) correlations are negligible. Above ξ_{corr} we can replace the bare random potential by a renormalized one that incorporates the effects of collective pinning. A second, more fundamental effect of the Coulomb interactions is that it fixes the lowest neutral excitation energy to be $E_0 \approx e^2/\epsilon\xi$ for an edge quasiparticle-quasihole pair. As a result, the dynamical exponent $z=1$. Coulomb interactions also introduce the possibility of inelastic tunneling in which a quasiparticle-quasihole pair is created when a quasihole tunnels across a saddle point. If we consider the propagation of a quasihole wave packet with energy within E_0 of μ , such incoherent processes can be ignored. In that case, the quasihole propagates through the network coherently as described above. At higher energies, inelastic processes will indeed destroy the coherence. Equivalently, only below a characteristic temperature, $T_0 = E_0/k_B$, will the coherent, zero-temperature physics determine the magnetotransport. The implication is that the thermal width of plateau transitions is determined by the condition $T = T_0(B)$ (i.e., $\kappa = 1/z\nu$), and hence $z_T = z = 1$, and $\kappa = \nu^{-1} \approx 0.42$ [12]. We stress that none of the effects of these interactions fundamentally alter the nature of the quantum percolation problem; in all cases, the plateau transition is driven by the delocalization of the edge quasiholes with energy μ . Interactions can affect the internal structure of the quasihole, and in the case of the fractional effect they can determine the charge and statistics of the quasihole, but they do not affect the character of the transition.

Now we present our numerical results. To demonstrate how quantum tunneling changes ν , we first set $W \rightarrow \infty$ and consider the classical problem. We have calculated ξ_M in a cylinder with $L = 2 \times 10^5$ and $M = 8 \rightarrow 128$ [13]. According to finite-size scaling, when $L \gg M$, ξ_M is given by $\xi_M(\mu)/M = F(\xi_\infty/M)$, where $\xi_\infty(\mu)$ is the thermodynamic localization length, and $F(x)$ is a scaling function. In Fig. 2 we present the scaling plot and $\ln(\xi_\infty)$ vs

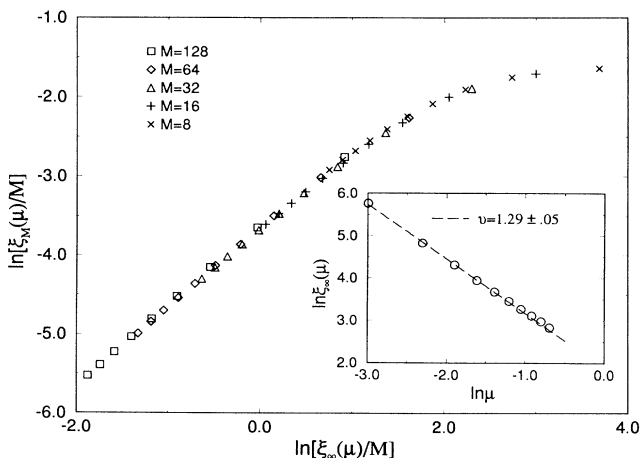


FIG. 2. The scaling plot for classical percolation. Inset: $\ln \xi_\infty$ vs $\ln \mu$.

$\ln(\mu)$. From these results, we obtained $\nu = 1.29 \pm 0.05$ consistent with the known classical percolation exponent $\nu_c = \frac{4}{3}$. Next we set $W=1$ and study the full quantum problem. In Fig. 3 we present the scaling plot and $\ln(\xi_\infty)$ vs $\ln(\mu)$. The quantum exponent we deduced from these results is $\nu = 2.43 \pm 0.18$, which is, within the error bars, consistent with $\nu = \frac{7}{3}$, the value that has been conjectured in [7(b)]. We have also studied several other values of W and found the same value for ν within numerical uncertainty.

To calculate the conductivities let us imagine a two-terminal geometry where a $M \times M$ network with periodic boundary conditions in the transverse direction is bounded on the left and right by two ideal "1" Hall liquids. In each of the ideal "leads" there is one incoming and one outgoing edge channel which is scattered by the "sample" in between. Because of current conservation, the effective transfer matrix characterizing the sample is a 2×2 matrix in the form of Eq. (1), where ϕ_i and γ are replaced by some yet unknown values $\phi_{i,\text{eff}}$ and γ_{eff} . To determine $\phi_{i,\text{eff}}$ and γ_{eff} , let us imagine diagonalizing the $M \times M$ transfer matrix and taking the modulus of the resulting eigenvalues. Among the mutual-reciprocal pairs let us single out the one $(|\lambda_0|, |\lambda_0|^{-1})$ (we assume $|\lambda_0| > 1$) where $|\lambda_0|$ is closest to unity.

The relation between $|\lambda_0|$ and γ_{eff} is given by $\ln(|\lambda_0|) = (M/\xi_M) = \gamma_{\text{eff}}$. The resulting effective transfer matrix can then be used to obtain a scattering matrix that links the incoming amplitudes (Z_1 and Z_2) with the outgoing amplitudes (Z_4 and Z_3). Under an appropriate choice of gauge the phases $\phi_{i,\text{eff}}$ can be absorbed and the S matrix takes the following form:

$$S = \begin{pmatrix} \tanh \gamma_{\text{eff}} & -\cosh^{-1} \gamma_{\text{eff}} \\ \cosh^{-1} \gamma_{\text{eff}} & \tanh \gamma_{\text{eff}} \end{pmatrix}. \quad (2)$$

From Eq. (2) we obtain the quasihole transmission coefficient $T = \cosh^{-2} \gamma_{\text{eff}}$ and the reflection coefficient

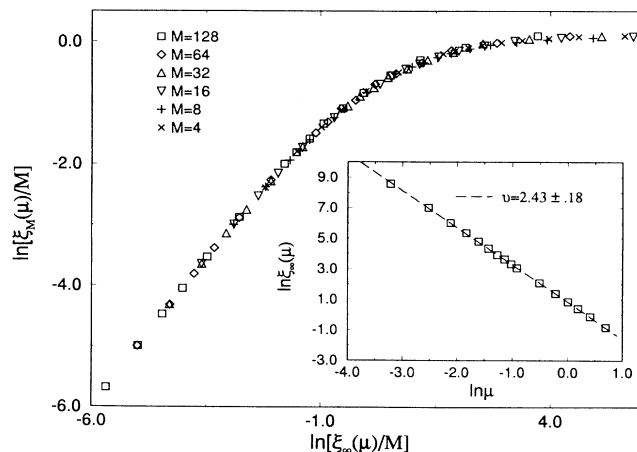


FIG. 3. The scaling plot for quantum percolation. Inset: $\ln \xi_\infty$ vs $\ln \mu$.

$R = \tanh^2 \gamma_{\text{eff}}$. From T and R we can compute the conductivity tensor in a Landauer-type approach. If all plateau transitions are governed by quasihole percolation, then T and R must assume universal scaling forms near the critical point. As a result, the following scaling relations connect the magnetotransport data of any pair (say a, b) of plateau transitions: Under conditions of fixed quasihole current $I = I_b/e_b^* = I_a/e_a^*$,

$$e_b^* V_{H,b} = e_a^* V_{H,a} + h(\theta_b - \theta_a)I, \quad e_b^* V_{L,b} = e_a^* V_{L,a}. \quad (3)$$

In the above, I_a , $V_{H,a}$, and $V_{L,a}$ are the quasihole *electrical* current, Hall voltage, and longitudinal voltage of the a th transition, respectively; e_a^* and θ_a are the charge and statistics [14] of the quasiholes that quantum percolate in the a th transition. To appreciate the physical origin of Eq. (3) we represent the quasihole associated with transition b as a particle with the statistics of the quasihole of transition a , with $\theta_b - \theta_a$ quanta of statistical flux attached to it to correct the statistics. Since the density operator is invariant under the operation of flux attachment, the transmission/reflection coefficient and the number current are independent of this flux. However, the associated flux current generates a *perpendicular* EMF, which makes an additive contribution to the effective Hall voltage [15] equal to Planck's constant times the flux current, $(\theta_b - \theta_a)I$. Therefore, if we choose a to be a reference integer plateau transition and use the Landauer formula $\rho_{xx} = (h/e^2)R/T$ and $\rho_{xy} = (h/e^2)$ to obtain the corresponding fermionic resistivity tensor [16], we obtain the following results for the resistivities of the anyons in transition b (we have dropped the subscript "b"):

$$\rho_{xx}^{qh} = \frac{h}{e^{*2}} \frac{R}{T}, \quad \rho_{xy}^{qh} = \frac{h}{e^{*2}} \theta. \quad (4)$$

By inverting the quasihole resistivity tensor we can compute the corresponding conductivities σ_{xx}^{qh} and σ_{xy}^{qh} . The total conductivity tensor is given by $\sigma_{xx} = \sigma_{xx}^{qh}$ and σ_{xy}

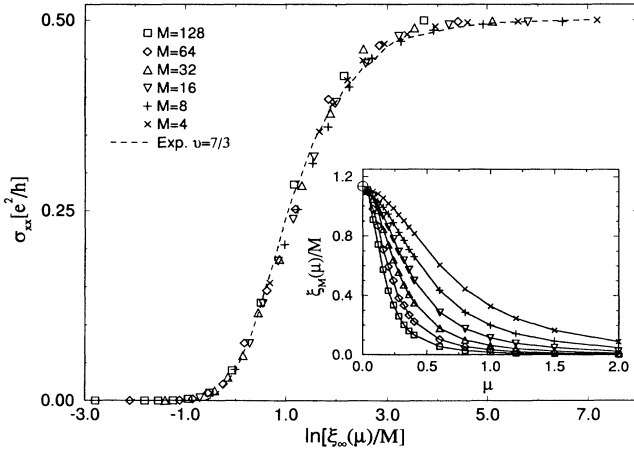


FIG. 4. The scaling plot for σ_{xx} . The dashed line is the experimental result of McEuen *et al.* [9] plotted using the exponent $\nu = \frac{7}{3}$. Inset: ξ_M/M vs μ . The open circle on the $\mu=0$ axis marks the position of γ_c^{-1} .

$= (e^2/h)(S_{xy} - \sigma_{xy}^{qh})$. Here $(e^2/h)S_{xy}$ is the Hall conductivity of the "1" Hall liquid. Putting everything together we get finally

$$\sigma_{xx} = \frac{e^*2}{h} \frac{\sinh^2 \gamma_{\text{eff}}}{1 + \theta^2 \sinh^4 \gamma_{\text{eff}}}, \quad (5)$$

$$\sigma_{xy} = \frac{e^2}{h} S_{xy} - \theta \frac{e^*2}{h} \frac{\sinh^4 \gamma_{\text{eff}}}{1 + \theta^2 \sinh^4 \gamma_{\text{eff}}},$$

where we have used $R/T = \sinh^2 \gamma_{\text{eff}}$. Equation (5) is in complete agreement with the result obtained by KLZ using the Chern-Simons approach [3]. We identify $\sinh^2 \gamma_{\text{eff}}$ in this work with the $\sigma_{xx}^{(b)}$ in Eq. (23) of Ref. [3(a)]. As γ_{eff} increases from 0 to ∞ the conductivity tensor evolves from $\sigma_{xy} = S_{xy}e^2/h$ and $\sigma_{xx} = 0$ to $\sigma_{xy} = S_{xy}e^2/h - e^*/h\theta$, $\sigma_{xx} = 0$. At the critical point $\gamma_{\text{eff}} = M/\xi_M \rightarrow \gamma_c = \ln(1 + \sqrt{2})$ (see the inset of Fig. 4) and the critical conductivities can be obtained from Eq. (5) by setting $\sinh \gamma_{\text{eff}} = 1$. For the integer quantum Hall effect $\theta = 1$, $e^* = e$ and $S_{xy} = \text{integer}$. In that case it follows that $\sigma_{xx}^c = e^2/2h$ and $\sigma_{xy}^c = (n - 1/2)e^2/h$ in agreement with [3(a)]. (Note also, as shown in KLZ, if we approach the transition from the other side in which we study the quantum percolation of the quasielectrons of the "0" Hall liquid, the same values of the critical conductivities are obtained.)

Away from the critical point, $\gamma_{\text{eff}} = M/\xi_M$ shows scaling behavior as a function of ξ_{∞}/M (Fig. 3) and the corresponding σ_{xx} vs $\ln(\xi_{\infty}/M)$ for the integer quantum Hall effect is shown in Fig. 4. Therefore, σ_{xx} should exhibit a universal scaling form in the transition region between quantized Hall plateaus. Extracting σ_{xx} from experimental data has to be performed with extreme care so that the edge current contribution from the parent ("0") Hall liquid is subtracted off. Such an analysis was done by McEuen *et al.* for the transition between the second

and the third integer Hall plateaus [9]. The dashed line in Fig. 4 is the data of McEuen *et al.* plotted as σ_{xx} vs $\ln(|B - B_c|^{-7/3})$; in making the comparison with the experimental data, we have identified $\xi_{\infty}(\mu)/M = (|B - B_c|/B_0)^{-7/3}$, where B_0 is the only adjustable parameter. The agreement with the data of McEuen *et al.* confirms that both the exponent and the critical conductivity are determined by quantum percolation.

We thank M. Inui, S. Sondhi, S. Trugman, X.-G. Wen, Y.-S. Wu, and especially S.-C. Zhang for many useful discussions. S.K. was supported in part by NSF Grant No. DMR-90-11803 at UCLA. Z.W. was supported by the U.S. Department of Energy.

- [1] See, e.g., *The Quantum Hall Effect*, edited by R. E. Prange and S. M. Girvin (Springer-Verlag, Berlin, 1990), 2nd ed.
- [2] R. B. Laughlin, Phys. Rev. Lett. **50**, 1395 (1983).
- [3] (a) S. A. Kivelson, D.-H. Lee, and S.-C. Zhang, Phys. Rev. B **46**, 2223 (1992); (b) D.-H. Lee, S. A. Kivelson, and S.-C. Zhang, Phys. Rev. Lett. **68**, 2386 (1992).
- [4] (a) A. M. M. Pruisken, Phys. Rev. Lett. **61**, 1297 (1988); (b) see, e.g., Chap. 5 in Ref. [1].
- [5] (a) H. P. Wei *et al.*, Phys. Rev. Lett. **61**, 1297 (1988); (b) L. Engel *et al.*, Surf. Sci. **229**, 13 (1990); (c) S. Koch *et al.*, Phys. Rev. Lett. **67**, 883 (1991).
- [6] (a) B. Huckestein and B. Kramer, Phys. Rev. Lett. **64**, 1437 (1990); D. Liu and S. Das Sarma (to be published); (b) Y. Huo, R. E. Hetzel, and R. N. Bhatt, Phys. Rev. Lett. **70**, 481 (1993).
- [7] (a) J. T. Chalker and P. D. Coddington, J. Phys. C **21**, 2665 (1988); (b) G. V. Mil'nikov and I. M. Sokolov, Pis'ma Zh. Eksp. Teor. Fiz. **48**, 494 (1988) [JETP Lett. **48**, 536 (1988)].
- [8] X.-G. Wen and A. Zee, Int. J. Mod. Phys. B **4**, 437 (1990); M. P. A. Fisher, G. Grinstein, and S. M. Girvin, Phys. Rev. Lett. **64**, 587 (1990).
- [9] P. L. McEuen *et al.*, Phys. Rev. Lett. **64**, 2062 (1990).
- [10] S. A. Trugman, Phys. Rev. B **27**, 7539 (1983).
- [11] As in Ref. [7(a)], we assume that due to the random phases of the quasiparticles at each saddle point, the difference between the topologies of a random network and a regular one can be ignored.
- [12] S. Sondhi and S. A. Kivelson (unpublished).
- [13] L is chosen such that the statistical errors in ξ_M are within 2%.
- [14] We choose the convention so that $\theta=0$ implies Bose and $\theta=1$ Fermi statistics.
- [15] See D.-H. Lee, in *Physics and Mathematics of Anyons*, edited by S. S. Chern, C. W. Chu, and C. S. Ting (World Scientific, Singapore, 1991).
- [16] P. Streda, J. Kucera, and A. H. MacDonald, Phys. Rev. Lett. **59**, 1973 (1987); J. K. Jain and S. A. Kivelson, Phys. Rev. Lett. **62**, 231 (1989); M. Buttiker, Phys. Rev. Lett. **62**, 229 (1989). We also note that the discrepancy between the results obtained by Buttiker and the others originates from the longitudinal and transverse mixing in the former.